Reducing Time Headway for Cooperative Vehicle Following in Platoon via Information Flow Topology

Nguyen Viet Hung * **Duc Lich Luu** ** **Ngo Sy Dong** *** **Ciprian Lupu** ****

* *Faculty of Information Technology, East Asia University of Technology, Hanoi 100000, Vietnam.*
** *Faculty of Transportation Mechanical Engineering, the University of Danang - University of Science and Technology, 54 Nguyen Luong Bang, Da Nang 550000, Vietnam.*
*** *Electric Power University, Hanoi 100000, Vietnam.*
**** *Department of Automatic Control and Systems Engineering, National University of Science and Technology POLITEHNICA Bucharest, Bucharest 060042, Romania.*
(Corresponding author: Duc Lich Luu, e-mail: ldlich@dut.udn.vn)

Abstract: For automated driving cars, Adaptive cruise control (ACC) systems of vehicular platoons are designed to provide longitudinal assistance for drivers to improve traffic throughput, enhance safety and reduce workload. As the core of all vehicular platoons, the information flow topology plays a crucial role in various aspects. In this study, we investigate the effects of information flow topology for connected and automated cars and provide results on how information flow topology helps reduce employable reducing time headway in platoons. String stability analysis of vehicular platoons has been validated via the Nyquist diagram. It is known that ACC vehicular platoons using a Constant Time Headway Spacing Strategy (CTH Strategy) and availing only embedded devices such as radar beam that need to maintain a high value of time headway for string stability. We show that if Cooperative Adaptive cruise control (CACC) vehicular platoons obtained acceleration of preceding car through the information flow topology that yields a smaller time headway value to maintain string stability. We provide numerical results to corroborate the results in this paper.

Keywords: Platooning, time headway, robust string stability, spacing strategy, cooperative control, V2V communication.

1. INTRODUCTION

The notion of Intelligent Vehicle Highway System (IVHS) was mentioned in the 1990s and has received special attention in the transportation engineering communities to accommodate exponentially increasing number of cars/trucks in today's life along with minimizing the risk of traffic accidents Swaroop et al. (2001). The primary strategy for implementing IVHS is to utilize automatic or semi-automatic systems for cars/trucks on highways, thereby reducing the need for human intervention in driving the cars/trucks.

Vehicle platooning, is one of the suitable applications of IVHS, which is a technique, in which IVHS is ganized into groups to drive closer with a smaller headway than normal cars/trucks with the same velocity called platoon or convoy. Platooning equipped with the ACC/CACC systems is not only a promising way to preventing traffic congestion, increase traffic capacity and safety, but can also reduce CO2 emissions Li et al. (2022). The ACC systems as a typical type of advanced driver assistance systems is an enhancement of the traditional cruise control (CC) systems Turan (2024). The ACC system stays a certain speed or a desired spacing with respect to the preceding car/truck by automatically adjusting actuators Luu and Lupu (2019). Then, advancements in V2V (Vehicle-to-Vehicle) channel and car control technology have made platooning feasible for partially automated cars, including the Cooperative Adaptive Cruise Control (CACC) system Wang et al. (2024).

One of the first ideas of organizing vehicles into platoons on highway to dramatically increase capacity is originally consider in Varaiya (1993) by PATH for IVHS, and was deployed successfully by National Automated Highway Systems Consortium employing eight vehicles in San Diego, CA, in 1997 Tan et al. (1998). A platoon consisting of a leading vehicle, which is usually the first vehicle in the platoon, followed closely by one or more subsequent followers. Platooning may be considered as an eco-driving strategy and is most effective for truck vehicles. It is considered as a solution to minimize fuel consumption of heavy duty vehicles Fahad and Nagy (2023).

The most important properties consist the local stability and string stability. Local stability is the general stability required for each individual car, and the spacing error between cars will converge to zero Feng et al. (2019). A local stability platoon is a string stable if the disturbance damps out when propagating to upstream cars, i.e. spacing errors are ensured not to amplify as they propagate towards the tail of the platoon, is essential for car platoons Tiganasu et al. (2021). The spacing errors of the following cars will be amplified more and more, called as string instability. String instability can even lead to a rear-end collision. Hence, for a platoon to be stable, it is not enough just to satisfy the local stability but also to satisfy the string stability. It is known that the string stability is highly influenced by the spacing policies. The most common spacing policies are the Constant Spacing Strategy (CS Strategy) Luu et al. (2022), Darbha et al. (2020) and the CTH Strategy Zhang et al. (2023), Li et al. (2019), Luu et al. (2022). A constant value defines the desired inter-car spacing in CS Strategy, which has the best potential to reduce the length of platoon and thus improve road throughput. While for CTH Strategy, the desired distance is a linear function of the velocity, with the proportional gain called time headway. We will focus on CTH Strategy in this paper, which agrees with human drivers' characteristics to some extent and has better applicability, potential to improve road capacity and safety.

In the case of the CS Strategy, string stability was presented in Luu et al. (2022) for CS Strategy with only radar sensors, laser or cameras, in Ghasemi et al. (2013) for CS Strategy under predecessor successor following (PF) topology, in Darbha et al. (2020) for CS Strategy under two-predecessor-leader following topology, in Barooah and Hespanha (2005) for CS Strategy under bidirectional topology. These studies provide valuable insights into the impact of V2V communication on platoons utilizing the CS Strategy. However, it is observed that string stability is still not achieved for platoons employing CS Strategy when using the infomation of predecessor. One potential solution for achieving string stability is to broadcast the leader's information, i,e the predecessor-leader following (PLF) topology Darbha et al. (2020). This is burdensome from the viewpoint of communication, especially when the platoon length grows.

Besides, there are other strategies that have been reported in the literature, such as Constant safety factor spacing policy Wu et al. (2020), semi-constant spacing strategy Zhang et al. (2020), and nonlinear spacing strategies Yanakiev and Kanellakopoulos (1998), these strategies have not attracted a lot of attention perhaps due to the complexity of the controller and the way it is implemented. For the CTH Strategy, string stability can be achieved without the dependence on the information of leader Ploeg et al. (2013), Rajamani (2011), Luu et al. (2019). Inside a platoon all the cars follow the leading car with the desired inter-car distance which corresponds to ACC/CACC time headway setting. The time headway setting of car is limited by string stability, traffic capacity, the traffic safety. Small time headway setting contributes to high throughput but can compromise the robustness of ACC/CACC platoon, i.e, it can be dangerous for the platoon, because it can bring to the local stability/string stability and, hence, collisions. In other words, an increase in time headway setting leads to a larger inter-car distance, which ensures safety, but the traffic capacity is reduced and the fuel/energy consumption is increased Nowakowski et al. (2016). The rapid advancement of communication techniques has expanded the possibilities for information flow topologies which provides benefits as well as challenges to design of CACC car control for platooning. The important open question is whether one can find the minimum acceptable time headway, which may ensure the string stability for the platoon, is of paramount importance. For this reason, we have investigated the benefits of V2V communication in terms of reduction in the minimum acceptable time headway for the CTH Strategy to guarantee the string stability, i.e, this value is significantly influenced by the information flow topology on platoons with the CTH Strategy.

The main contribution of this paper involves demonstrating that the benefits of any information of the V2V communication topology in connected and autonomous cars. We consider CACC cars form a car platoon under the predecessor-following (PF) topology, when both on-board sensors and V2V communication are used, PF information flow is commonly used in platooning applications because of its relatively low communication overhead and simplicity. And ACC cars form a car platoon can only gather information through radar or onboard sensors. The platoon leader is assumed to follow the Urban Dynamometer Driving Schedule by means of a CC system. The other cars of the platoon pursue each other closely with the desired inter-car distance. namely: (i) the string stability of the platoon are rigorously proved by utilizing the Nyquist region. The time headway optimization is considered with different values through the Nyquist diagram. According to this, the minimum time headway have been investigated in two case of platoons, including ACC cars and CACC cars, we has been proved that by using the V2V communication, the minimum acceptable time headway will be reduced; (ii). to show this, a simulation for connected car applications was implemented to provide the proof again of string stability through the propagation of disturbance in a string of cars. Simultaneously, verify the effectiveness and advantage of the developed platoon controller.

The outline of the rest of the paper is as follows. Section II is presented the problem for formulation. The controller structure, string stability analysis is introduced in Section III. The simulation results based on MATLAB from nine car convoy are presented in Section IV. The paper ends with conclusions and directions for future work in the last section.

2. PROBLEM FORMULATION

Fig.1 presents a specific platoon scenario of $N+1$ of queued cars consisting of one leader ($i=0$) and N followers ($i=1,\dots,N$). In this study, we consider first platoon of cars are equipped the ACC system, each ACC car are equipped with devices to measure the distance, relative velocity to the preceding car, and second platoon of cars are equipped the CACC system, in which each followers shares its acceleration with the following cars via a PF communication network consisting of multiple redundant channels. The information flow topology relies on the information provided by the car directly ahead of it, this reduces burdensome from the viewpoint of communication as the platoon length grows. It is assumed that the network experiences no packet loss due to the implementation of multi-channel transmission.

2.1 Vehicle Dynamics

The car dynamics has been determined by engine, drive line, brake system, tire fraction, aerodynamics drag, gravitational force, and rolling resistance etc. To simplify understanding, some general assumptions were introduced to construct the model in this paper. The general assumptions are listed as follows:

A1: Longitudinal tire slip in each car is not considered.

A2: The car body is considered to be rigid and symmetric.

A3: The car platoon travels in one dimension, which is, only motion in the longitudinal direction is considered.

A4: The controller for all followers in the platoon uses information from both the leader and the preceding car.

A5: The leader car is controlled by the CC system with the reference of the closed-loop system is the desired reference speed.

The dynamics of the following car i can be described by the following nonlinear differential equations Wu et al. (2021), Rajamani (2011):

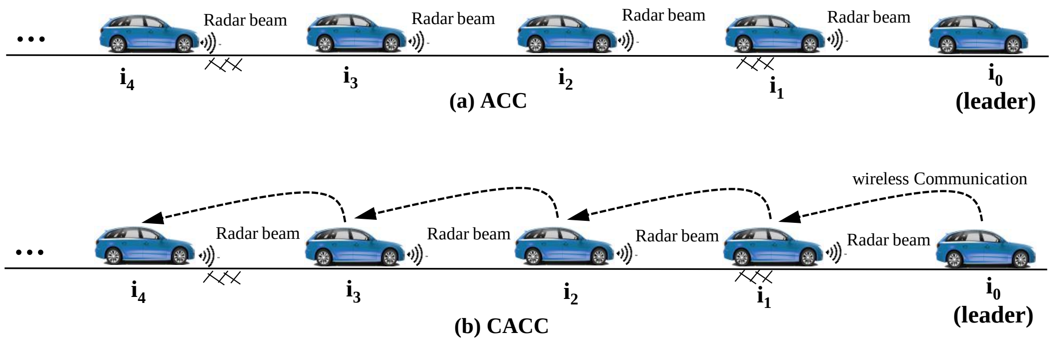

Fig. 1. Examples of a platoon

$$\begin{cases} \dot{p}_i(t) = v_i(t) \\ \ddot{p}_i(t) = a_i(t) \\ \dot{a}_i(t) = f_i(v_i(t), a_i(t), t) + g_i(v(t))\chi_i(t), \quad i = \overline{1, N}, \end{cases} \tag{1}$$

where $p_i(m)$, $v_i(m/s)$, $a_i(t)$ indicates the position, velocity, acceleration in longitudinal axis of the car i, corresponding

$\chi_i(t)$ is the engine input, and g_i is given as

$$g_i(v_i(t)) = \frac{1}{\varsigma_i m_i} \tag{2}$$

where m_i is mass of the car i. The above model is nonlinear due to the nonlinear function $f_i(v_i(t), a_i(t), t)$ described as:

$$f_i(v_i(t), a_i(t), t) = -\frac{1}{\varsigma_i}\dot{v}_i - \frac{1}{\varsigma_i m_i}\Big(\frac{\delta A_i f_{di}}{2m_i} v_i^2 + p_{mi} + \delta A_i f_{di} v_i a_i\Big) \tag{3}$$

where ς_i is engine time constant of car (also called the inertial time-lag), p_{mi} indicates the mechanical drag, f_{di} denotes the drag coefficient, δ is the air density, A_i represents the cross-sectional area, and the group of terms $\frac{\delta A_i f_{di}}{2m_i}$ standing for the air resistance Ghasemi et al. (2013).

Remark: The inertial time-lag ς_i in equation can be determined by the model identification procedure proposed by Li et al. (2017) empoying driving conditions and the parameters. The range of the obtained motor time constant is 0.32s to 0.82s in Li et al. (2017) using Matlab's Toolbox.

Several literatures on platoon control problems have utilized simplified car models, such as double integrator dynamics or other simplified models Pi et al. (2023). However, it has been recognized that the control structure based on these simplified models can not be sufficient to handle the complex nonlinear dynamics exhibited by real cars. To address this limitation, the complete nonlinear model of car-like cars equation (1) is considered for controller design, taking into account the intricacies of the nonlinear dynamics involved.

According to the feedback linearisation technology, we adopt the following control law as shown in Godbole and Lygeros (1994), Stankovic et al. (2000), Guo and Yue (2012):

$$\chi_i(t) = u_i m_i + \frac{\delta A_i f_{di}}{2} v_i^2 + p_{mi} + \delta A_i f_{di} v_i a_i \tag{4}$$

where the new control u_i is the input signal of car i to be designed so that the closed-loop system can satisfy certain performance criteria (also called the desired acceleration). By substitutin equation (2), (3), (4) into the third equation in (equation (1), we derive a three-order linearized model that is used to represent the longitudinal dynamics of the car, i.e.

$$\varsigma_i \dot{a}_i(t) + a_i(t) = u_i(t) \tag{5}$$

which is then expressed in the standard state-space form as

$$\dot{\mathbf{X}}_{v,i} = \mathbf{A}_{v,i} X_i + \mathbf{b}_{v,i} u_i \tag{6}$$

where

$$\mathbf{A}_{v,i} = \begin{bmatrix} 0 & 1 & 0 \\ 0 & 0 & 1 \\ 0 & 0 & -\frac{1}{\varsigma_i} \end{bmatrix}; \mathbf{b}_{v,i} \begin{bmatrix} 0 \\ 0 \\ \frac{1}{\varsigma_i} \end{bmatrix}; X_{v,i} = [p_i \ \ v_i \ \ a_i]^T$$

Simplified model of the complexity modeling the longitudinal dynamics of the car. Note that, the linear model equation (1) fully describes the longitudinal dynamics of acceleration-controlled cars through experimental validation and has been widely applies to design the CACC controller of platoons Öncü et al. (2014).

The linear model equation (5) has been used as the upper level controller in the structure of ACC system, e.g., Öncü et al. (2014), He and Peng (2020). In this control structure, the nonlinear model equation (4) is seen as the lower level controller of car and commonly used for design in complete CACC system although component $\frac{\delta A_i f_{di}}{2m_i}$ is often difficult to estimate perfectly due to the unknown drag coefficient Orosz (2016). In this study, we focus ourselves on the upper level controller in Equation (3) by assuming the desired control performance of the lower level controller of cars.

2.2 Car Platoon System

In a platoon system study, the platoon control's target is to track the velocity of the leader, while to keep a formation governed by the desired spacing strategy between any two consecutive following cars. When using a CS Strategy Guo and Yue (2014) , it is important to maintain a small, hence it can achieve higher traffic efficiency Luu et al. (2022). However, the issue of safety between cars during travel is a major challenge for this strategy. In the CTH Strategy, the distance follows a linear relationship with self-velocity, the distance between the two consecutive cars is larger, so it is safer. However, it can not significantly improve the traffic capacity as high as the CS strategy. For this reason, the CTH strategy is applied for platoon control design in this paper to improve the traffic capacity for this CTH strategy.

The desired spacing in the platoon system is not constant. In fact, it has a linear relationship with the speed, and it has an introduced time headway parameter h_i as shown in the following equation:

$$D_{des,i}(t) = c_0 + h_i \dot{p}_i(t) \tag{7}$$

where, $D_{des,i}(t)$ is the desired inter-car spacing, c_0 is a positive space constant, which represents the static distance when car stop, h_i is the headway time.

The real spacing between any two consecutive following cars:

$$D_i(t) = p_{i-1}(t) - p_i(t) - L_{i-1} \tag{8}$$

where L_{i-1} is the length of car $i-1$. The spacing error for car i is given by the difference of real spacing and the desired spacing as:

$$\varepsilon_i(t) = D_i(t) - c_0 - h_i \dot{p}_i(t) \tag{9}$$

2.3 Objectives

This paper goals to derive a cooperative control method for a group of cars driving in platoon, for follower cars so that the following two objectives are satisfied.

- Closed-loop stability:

All the follower cars tend to travel at the same speed as the leader car and the spacing error of the following car converge to zero, namely:

$$\begin{cases} \lim\limits_{t\to\infty} \|D_i(t) - c_0 - h_i \dot{p}_i(t)\| \to 0 \\ \lim\limits_{t\to\infty} \|v_i(t)\| \to v_0(t) \end{cases} \tag{10}$$

- String stability:

The spacing error of the following car are not amplified during the backward propagation along the platoon, namely:

$$\sup_{t\to\infty} \left|\frac{\varepsilon_i(j\omega)}{\varepsilon_{i-1}(j\omega)}\right| \leq 1, \quad i = \overline{1,N}, \quad \forall\omega \in \mathbb{R}^+ \tag{11}$$

3. CONTROLLER STRUCTURE

The ACC system considering the information flow topology is one of the subsystem of the Advanced Driver Assistance System. The follower cars equipped with the ACC system is to maintain the same speed as the leader while keeping the desired distance to the corresponding preceding car defined by the spacing policy. The spacing policy is chosen the CTH strategy. The transfer function between adjacent cars will be derived, then the Nyquist region of string stable systems and string stability analyses will be discussed subsequently.

3.1 The design of ACC system based on CTH Strategy

The state equation of the ACC system based CTH strategy can be written as shown in equation (12) where x is the state matrix:

$$\begin{cases} \dot{x}_1 = \dot{\varepsilon}_i = \Delta v_i + h_i a_i \\ \dot{x}_2 = \Delta \dot{v}_i = a_{i-1} - a_i \\ \dot{x}_3 = \dot{a}_i = \dfrac{-1}{\varsigma_i} a_i + \dfrac{-1}{\varsigma_i} u_i \end{cases} \tag{12}$$

Defining the state vector:

$$\mathbf{x}_i = [\varepsilon_i \;\; \Delta v_i \;\; a_i]^T$$

The equation (12) can be rewritten in the linear time-invariant (LTI) state-space representation as:

$$\dot{\mathbf{x}}_i = \mathbf{A}_i x_i + \mathbf{B}_i u_i + \mathbf{G}_i w_i \tag{13}$$

where $\mathbf{A}_i$, $\mathbf{B}_i$, $\mathbf{G}_i$ are the model matrices of appropriate dimensions, and $w_i = [a_{i-1}]$ as system disturbance.

$$\mathbf{A}_i = \begin{bmatrix} 0 & 1 & -h_i \\ 0 & 0 & -1 \\ 0 & 0 & \dfrac{-1}{\varsigma_i} \end{bmatrix}; \mathbf{B}_i = \begin{bmatrix} 0 \\ 0 \\ \dfrac{1}{\varsigma_i} \end{bmatrix}; \mathbf{G}_i = \begin{bmatrix} 0 \\ 1 \\ 0 \end{bmatrix}$$

For controller design, it is assumed that all the states are available from measurements or can be estimated. Let us consider the feedback control law:

$$u_i = -\mathbf{K}_i \mathbf{x}_i = \kappa_1 \varepsilon_i + \kappa_2 \Delta v_i + \kappa_3 a_i \tag{14}$$

where $\mathbf{K}_i$ is the state feedback gain matrix, the coefficients κ_1 to κ_3 are the elements of the gain matrix $\mathbf{K}_i$. The optimisation procedure consists in determining the control input u_i which minimises some performance index $J(x_i, u_i)$. A control index function considering car distance, relative speed, and main car acceleration, usually expressed by:

$$J(\mathbf{x}_i, u_i) = \int_0^\infty (\mathbf{x}_i^T \mathbf{Q} \mathbf{x}_i + u_i^T \mathbf{R} u_i)\, d\tau \tag{15}$$

where $Q = Q^T \geqslant 0$ and $R = R^T \geqslant 0$ are positive definite weighting matrices. In order to find an optimal controller solution for Eq.14, the linear time-invariant system must be stabilizable. This condition holds true for the system described in Eq.13. Based on the LQR control theory, the gain K_i minimizing Eq.21 has the following form:

$$K_i = \mathbf{R}^{-1} \mathbf{B}^T \mathbf{P} \tag{16}$$

where the matrix $\mathbf{P}$ is the solution of the algebraic Riccati equation:

$$\mathbf{A}_i^T \mathbf{P} + \mathbf{P} \mathbf{A}_i - \mathbf{P} \mathbf{B} \mathbf{R}^{-1} \mathbf{B}^T \mathbf{P} + \mathbf{Q} = 0 \tag{17}$$

The performance index $J(x_i, u_i)$ in equation (15) is then selected as follows:

$$J(\mathbf{x}_i, u_i) = \int_0^\infty (\rho_1 \varepsilon_i^2 + \rho_2 \Delta v_i^2 + \rho_3 a_i + r_1 u_i^2)\, d\tau \tag{18}$$

where ρ_1, ρ_2, and ρ_3 are the weight coefficients of distance error of car, relative velocity, and main car acceleration, respectively; r_1 is the weight coefficient limiting the jitter of the expected acceleration.

3.2 The design of CACC system based on CTH Strategy With PF Scheme

ACC automatically adjusts the speed of a car in the presence of preceding traffic. Typically, radar or lidar is employed to detect the preceding traffic, facilitating the automatic following of a predecessor. Extending ACC functionality with wireless inter-car communication is called CACC. Thus, the CACC system use predecessor acceleration feedback in the controller. The state equation of the CACC system based CTH strategy can be written as shown in equation (12) where x is the state matrix:

$$\begin{cases} \dot{\tilde{x}}_1 = \dot{\tilde{\varepsilon}}_i = \Delta\tilde{v}_i + h_i\tilde{a}_i \\ \dot{\tilde{x}}_2 = \Delta\dot{\tilde{v}}_i = \tilde{a}_{i-1} - \tilde{a}_i \\ \dot{\tilde{x}}_3 = \dot{\tilde{a}}_i = \dfrac{-1}{\tilde{\varsigma}_i}\tilde{a}_i + \dfrac{-1}{\tilde{\varsigma}_i}\tilde{u}_i \\ \dot{\tilde{x}}_4 = \dot{\tilde{a}}_{i-1} = \dfrac{-1}{\tilde{\varsigma}_{i-1}}\tilde{a}_{i-1} + \dfrac{-1}{\tilde{\varsigma}_{i-1}}\tilde{u}_{i-1} \end{cases} \tag{19}$$

$$\Rightarrow \dot{\tilde{\mathbf{x}}}_i = \tilde{\mathbf{A}}_i\tilde{x}_i + \tilde{\mathbf{B}}_i\tilde{u}_i + \tilde{\mathbf{G}}_i\tilde{w}_i \tag{20}$$

Considering the worst scenario, i.e., the case of maximum delay θ, the finalized feedback control for the followers with LQR gain $\tilde{\mathbf{K}}_i$ is shown as:

$$\begin{aligned} \tilde{u}_i &= -\tilde{\mathbf{K}}_i\tilde{\mathbf{x}}_i \\ &= \tilde{\kappa}_1\tilde{\varepsilon}_i(t-\theta) + \tilde{\kappa}_2\Delta\tilde{v}_i(t-\theta) + \tilde{\kappa}_3(\tilde{a}_i(t-\theta) - \tilde{a}_{i-1}(t-\theta)) \end{aligned} \tag{21}$$

where $\tilde{\mathbf{K}}_i$ is the state feedback gain matrix, the coefficients $\tilde{\kappa}_1$ to $\tilde{\kappa}_4$ are the elements of the gain matrix $\tilde{\mathbf{K}}_i$, and $\tilde{\mathbf{x}}_i = [\tilde{x}_1 \quad \tilde{x}_2 \quad \tilde{x}_3 \quad \tilde{x}_4]^T$, $\tilde{w}_i = [\tilde{a}_{i-1}]$ as system disturbance.

The optimization procedure consists in determining the control input $\tilde{u}_i$ which minimizes some performance index $\tilde{J}(\tilde{u}_i, \tilde{x}_i)$. This index includes the performance characteristic requirement as well as the controller input limitations, usually expressed by.

$$\tilde{J}(\tilde{\mathbf{x}}_i, \tilde{u}_i) = \int_0^\infty (\tilde{\rho}_1\tilde{\varepsilon}_i^2 + \tilde{\rho}_2\Delta\tilde{v}_i^2 + \tilde{\rho}_3\tilde{a}_i + \tilde{r}_1\tilde{u}_i^2)\,d\tau \tag{22}$$

where $\tilde{\rho}_1$, $\tilde{\rho}_2$, $\tilde{\rho}_3$ and $\tilde{\rho}_4$ are the weight coefficients of distance error of car, relative velocity, and main car acceleration, respectively; $\tilde{r}_1$ is the weight coefficient limiting the jitter of the expected acceleration. From the linear optimal control theory,the minimum expected car following acceleration of $\tilde{J}(\tilde{\mathbf{x}}_i, \tilde{u}_i)$ is sought.

3.3 String Stability Analysis

In this section, the transfer functions of the spacing errors between adjacent cars is established and then present the string stability criterion.

- Transfer function of the spacing errors:

In order to determine the transfer function of spacing errors between the car i and its preceding car for the ACC system, it is initially considered the spacing error:

$$\varepsilon_i(t) = p_{i-1}(t) - p_i(t) - L_{i-1} - c_0 - h_i\dot{p}_i(t) \tag{23}$$

The time derivative of the spacing error, we get:

$$\begin{aligned} &\dot{\varepsilon}_i = \dot{p}_{i-1} - \dot{p}_i - h_i\ddot{p}_i \Rightarrow \dot{p}_i = \dot{p}_{i-1} - \dot{\varepsilon}_i - h_i\ddot{p}_i \\ &\ddot{\varepsilon}_i = \ddot{p}_{i-1} - \ddot{p}_i - h_i\dddot{p}_i \Rightarrow \ddot{p}_i = \ddot{p}_{i-1} - \ddot{\varepsilon}_i - h_i\dddot{p}_i \\ &\dddot{\varepsilon}_i = \dddot{p}_{i-1} - \dddot{p}_i - h_i\ddddot{p}_i \Rightarrow \dddot{p}_i = \dddot{p}_{i-1} - \dddot{\varepsilon}_i - h_i\ddddot{p}_i \end{aligned} \tag{24}$$

Bring the equation (24) into equation (6), it becomes:

$$\begin{aligned} \varsigma_i\dddot{p}_{i-1} + \ddot{p}_{i-1} - h_i(\varsigma_i\ddddot{p}_i + \dddot{p}_i) - u_i &= \varsigma_i\dddot{\varepsilon}_i + \ddot{\varepsilon}_i \\ \Rightarrow u_{i-1} - h_i\dot{u}_i - u_i &= \varsigma_i\dddot{\varepsilon}_i + \ddot{\varepsilon}_i \end{aligned} \tag{25}$$

Replace the equation (14) into the equation (25):

$$\begin{aligned} &\kappa_1\varepsilon_{i-1} - \kappa_1 h_i\dot{\varepsilon}_i - \kappa_1\varepsilon_i + \kappa_2(\dot{p}_{i-2} - \dot{p}_{i-1} - h_i\ddot{p}_{i-1}) \\ &- \kappa_2(\dot{p}_{i-1} - \dot{p}_i - h_i\ddot{p}_i) + \kappa_3(\ddot{p}_{i-1} - \ddot{p}_i - h_i\dddot{p}_i) = \varsigma_i\dddot{\varepsilon}_i + \ddot{\varepsilon}_i \\ &\Rightarrow \kappa_1\varepsilon_{i-1} - \kappa_1 h_i\dot{\varepsilon}_i - \kappa_1\varepsilon_i + \kappa_2\dot{\varepsilon}_{i-1} - \kappa_2\dot{\varepsilon}_i + \kappa_3\ddot{\varepsilon}_i \\ &= \varsigma_i\dddot{\varepsilon}_i + \ddot{\varepsilon}_i \end{aligned} \tag{26}$$

Gives the transfer function equation as follows:

$$\Phi_i(s) = \frac{\kappa_2 s + \kappa_1}{\varsigma_i s^3 + (1-\kappa_3)s^2 + (\kappa_2 + h_i\kappa_1)s + \kappa_1} \tag{27}$$

where $\Phi_i(j\omega)$ is the Laplace transform of $\varepsilon_i(t)$.

Now, we are ready to introduce Theorem 1, detailing the conditions for string stability.

Theorem 1: For any scalar $\omega > 0$, the string stability of the ACC systems can be achieved under the platoon control law equation (14), if all the following conditions are satisfied:

$$h_i \geq \frac{2\varsigma_i}{(1-\kappa_3)^2} \tag{28}$$

Proof. See Appendix A

In order to determine the transfer function of spacing errors between the car i and its preceding car for the CACC system, it is initially considered the spacing error:

$$\tilde{\varepsilon}_i = \tilde{p}_{i-1} - \tilde{p}_i - L_{i-1} - c_0 - h_i\dot{\tilde{p}}_i \tag{29}$$

The following third derivative of the equation (29) can be derived:

$$\begin{aligned} &\dot{\tilde{\varepsilon}}_i = \dot{\tilde{p}}_{i-1} - \dot{\tilde{p}}_i - h_i\ddot{\tilde{p}}_i \Rightarrow \dot{\tilde{p}}_i = \dot{\tilde{p}}_{i-1} - \dot{\tilde{\varepsilon}}_i - h_i\ddot{\tilde{p}}_i \\ &\ddot{\tilde{\varepsilon}}_i = \ddot{\tilde{p}}_{i-1} - \ddot{\tilde{p}}_i - h_i\dddot{\tilde{p}}_i \Rightarrow \ddot{\tilde{p}}_i = \ddot{\tilde{p}}_{i-1} - \ddot{\tilde{\varepsilon}}_i - h_i\dddot{\tilde{p}}_i \\ &\dddot{\tilde{\varepsilon}}_i = \dddot{\tilde{p}}_{i-1} - \dddot{\tilde{p}}_i - h_i\ddddot{\tilde{p}}_i \Rightarrow \dddot{\tilde{p}}_i = \dddot{\tilde{p}}_{i-1} - \dddot{\tilde{\varepsilon}}_i - h_i\ddddot{\tilde{p}}_i \end{aligned} \tag{30}$$

Combining with $\varsigma_i\dddot{\tilde{p}}_i + \ddot{\tilde{p}}_i = \tilde{u}_i$ in longitudinal car model (5), we have:

$$\tilde{u}_{i-1} - h_i\dot{\tilde{u}}_i - \tilde{u}_i = \varsigma_i\dddot{\tilde{\varepsilon}}_i + \ddot{\tilde{\varepsilon}}_i \tag{31}$$

Replace the equation (21) into the equation (31):

$$\begin{aligned} &\tilde{\kappa}_3[\ddot{\tilde{p}}_{i-2}(t-\theta) - \ddot{\tilde{p}}_{i-1}(t-\theta) - h_i\dddot{\tilde{p}}_{i-1}(t-\theta)] \\ &+ \tilde{\kappa}_3[\ddot{\tilde{p}}_{i-1}(t-\theta) - \ddot{\tilde{p}}_i(t-\theta) - h_i\dddot{\tilde{p}}_i(t-\theta)] \\ &+ \tilde{\kappa}_2[\dot{\tilde{p}}_{i-2}(t-\theta) - \dot{\tilde{p}}_{i-1}(t-\theta) - h_i\ddot{\tilde{p}}_{i-1}(t-\theta)] \\ &- \tilde{\kappa}_2[\dot{\tilde{p}}_{i-1}(t-\theta) - \dot{\tilde{p}}_i(t-\theta) - h_i\ddot{\tilde{p}}_i(t-\theta)] \\ &+ \tilde{\kappa}_1\tilde{\varepsilon}_{i-1}(t-\theta) - \tilde{\kappa}_1 h_i\dot{\tilde{\varepsilon}}_i(t-\theta) - \tilde{\kappa}_1\tilde{\varepsilon}_i(t-\theta) = \varsigma_i\dddot{\tilde{\varepsilon}}_i \\ &+ \ddot{\tilde{\varepsilon}}_i \Rightarrow \tilde{\kappa}_3\ddot{\tilde{\varepsilon}}_{i-1}(t-\theta) - \tilde{\kappa}_3\ddot{\tilde{\varepsilon}}_i(t-\theta) + \tilde{\kappa}_2\dot{\tilde{\varepsilon}}_{i-1}(t-\theta) \\ &- \tilde{\kappa}_2\dot{\tilde{\varepsilon}}_i(t-\theta) + \kappa_1\tilde{\varepsilon}_{i-1}(t-\theta) - \tilde{\kappa}_1 h_i\dot{\tilde{\varepsilon}}_i(t-\theta) - \tilde{\kappa}_1\tilde{\varepsilon}_i(t-\theta) \\ &= \varsigma_i\dddot{\tilde{\varepsilon}}_i(t) + \ddot{\tilde{\varepsilon}}_i(t) \end{aligned} \tag{32}$$

Using the Laplace transformation to equation (32), the transfer function of spacing error propagation is obtained as follows:

$$\tilde{\Phi}_i(s,\theta) = \frac{(\tilde{\kappa}_3 s^2 + \tilde{\kappa}_2 s + \tilde{\kappa}_1)e^{-\theta s}}{\tilde{\varsigma}_i s^3 + s^2 + [\tilde{\kappa}_3 s^2 + (\tilde{\kappa}_2 + h_i\tilde{\kappa}_1)s + \tilde{\kappa}_1]e^{-\theta s}} \tag{33}$$

We see that compared to the transfer function (33) of the ACC system, the CACC system has a non-zero acceleration feedback gains κ_3.

According to the transfer function function (33), a set of sufficient conditions for string stability is derived in Theorem 2.

Theorem 2: For any scalar $\omega > 0$, the string stability of the CACC systems can be achieved under the platoon control law equation (21), if the following sufficient condition hold:

$$h_i \geq \frac{2(\varsigma_i + \theta)}{2\tilde{\kappa}_3 + 1} \tag{34}$$

then, string stability can be guaranteed.

Proof. See Appendix B.

- String Stability Criterion:

Definition1 (L_2 String Stability): A car platoon by a linear time-invariant systems is said to be strictly L_2 string stable if:

$$\|\Phi_i(j\omega)\| \leq 1 \tag{35}$$

$$\|\tilde{\Phi}_i(j\omega, \theta)\| \leq 1 \tag{36}$$

Next, we propose and prove a Nyquist region mapping theorem of a string stable system in the complex plane.

Theorem 3: (Nyquist region of string stable systems Mokogwu and Hashtrudi-Zaad (2022)): Given the linear time-invariant system

$$Y_i(s) = \Phi_i X_i(s) \tag{37}$$

indicating a single sub-system of platoon containing n inter-connected subsystems with U_i-input, Y_i-output and Φ_i-transfer function, with no poles in the complex right-half-plane. The condition is

$$(\Re[\Phi(j\omega)])^2 + (\Im[\Phi(j\omega)])^2 \leq 1 \tag{38}$$

for each sub-system is a condition for string stability, with $\Re[\Phi(j\omega)]$ and $\Im[\Phi(j\omega)]$ represent the real and complex parts of their arguments.

Proof of Theorem 3: Consider the definition of string stability

$$\|z_i\|_2 \leq \|z_{i-1}\|_2 \tag{39}$$

Suppose that z_i and z_{i-1} are the input and output of subsystem in the car platooning. The variables z_{i-1} and z_i are replaced by the input x and output y respectively. Squared both sides of equation (39) gives a two-norm definition of input and output signals:

$$\|y\|_2^2 \leq \|x\|_2^2 \;\Rightarrow \int_0^t |y|^2\, dt \leq \int_0^t |x|^2\, dt \tag{40}$$

Using Parseval's theorem for equation (40), the time integration must be over $t \in (-\infty, +\infty)$. So, the truncation operator given in (8) is employed. Using Parseval's theorem to both sides of (13) yields

$$\int_0^t |y|^2\, dt = \int_{-\infty}^{+\infty} |y_\tau|^2\, d\tau = \frac{1}{2\pi} \int_{-\infty}^{+\infty} |\Phi(j\omega)|^2\, |X_\tau(j\omega)|^2\, d\omega \tag{41}$$

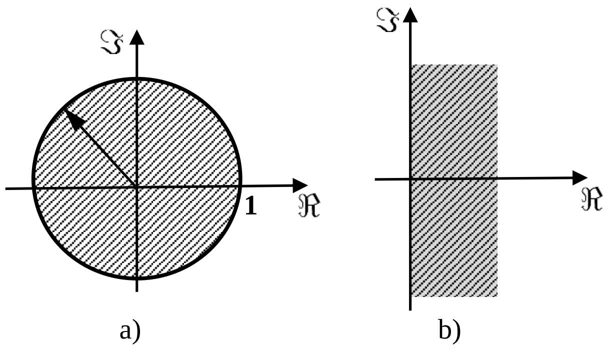

Fig. 2. Nyquist regions of (a) String stable region, (b) Passivity region in the complex plane.

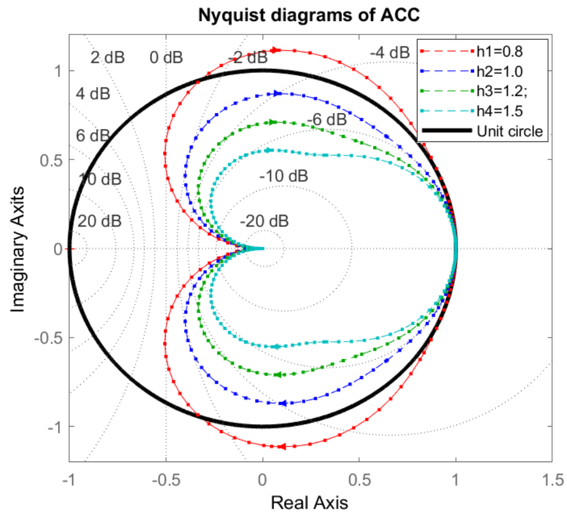

Fig. 3. ACC system with different values of headway time h_i

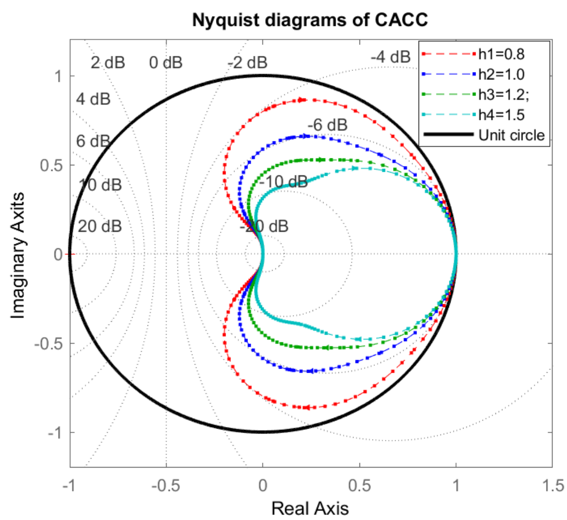

Fig. 4. CACC system with different values of headway time h_i

in which $Y(j\omega) = \Phi(j\omega)X_\tau(j\omega)$ lead to

$$\int_0^t |x|^2\,dt = \int_{-\infty}^{+\infty} |x_\tau|^2\,d\tau = \frac{1}{2\pi}\int_{-\infty}^{+\infty} |U_\tau(j\omega)|^2\,d\omega \qquad (42)$$

Substituting equation (41) equation (42) into equation (40), we have

$$\int_{-\infty}^{+\infty} |\Phi(j\omega)|^2\,|X_\tau(j\omega)|^2\,d\omega \le \int_{-\infty}^{+\infty} |U_\tau(j\omega)|^2\,d\omega \qquad (43)$$

It is straightforward to observe that $|\Phi(j\omega)|^2 \le 1$ is a condition for the above inequality to hold. Therefore, the condition:

$$|\Phi(j\omega)|^2 = (\Re[\Phi(j\omega)])^2 + (\Im[\Phi(j\omega)])^2 \le 1 \qquad (44)$$

seeing that the Nyquist plot of $\Phi(j\omega)$ is within the the unit circle in the complex plane, is sufficient for string stability.

Theorem 1 demonstrates that if the Nyquist region of all subsystems in the car platooning are bounded by the unit circle with its center at the origin of the coordinate plane, as shown in Fig.2, then the L_2 string stability is ensured.

Next, we use the Nyquist diagram to evaluate the string stability. The time headway is considered with different values $h_i = [0.8; 1.0; 0.9; 1.2; 1.5]s$. For the ACC system, we observe that time headway $h_i = 0.8s$ less than the minimum time headway then the string stability becomes unstable. The unstable string stability is indicated by the Nyquist diagram as in Fig.3 where the line exceeded the unit circle. It means that the spacing errors are amplified in the platoon.

For the CACC system, the different values of time headway brings the string stability. It correlated to the Nyquist diagram as shown in Fig.4. All lines are inside the unit circle, i.e, the spacing errors are attenuated from the front to the back along the platoon.

Finally, we will verify the string stability for both ACC system with $h_i = 1.05s$ and CACC system with $h_i = 0.8s$ by Numerical simulation.

4. SIMULATION RESULTS BASED ON MATLAB

4.1 Numerical simulation design and parameter selection

In this section, we conduct a comparative study to showcase the effectiveness and advantages of the proposed event-triggered platoon control algorithm, when consider a scenario in which a set of identical cars grouped as a homogeneous platoon are moving in a city and on a highway with the speed reference of leader car employed in this simulation study is the typical driving cycle that is a Urban Dynamometer Driving Schedule - UDDS (Zhou et al. (2020)) shown in Fig.5.

The controller gain matrix $\mathbf{K}_i$, $\tilde{\mathbf{K}}_i$ for both controller ACC and CACC can be computed delay the Riccati equation (17). The platoon common parameters as follow: $\varsigma_i = 0.5s$, $c_0 = 2m$, $\theta = 0.005s$, $L = 5m$, p_i at $t = 0s$ are $[0; 7; 14; 21; 28; 35; 42; 49; 56]m$ ACC specific platoon parameters as follow: $\mathbf{K}_i = [0.8; 2; 0.05]$, $h_i = 1.05s$ and CACC specific platoon parameters as follow: $\tilde{\mathbf{K}}_i = [0.8; 2; 0.25; 0.25]$, $h_i = 0.8s$.

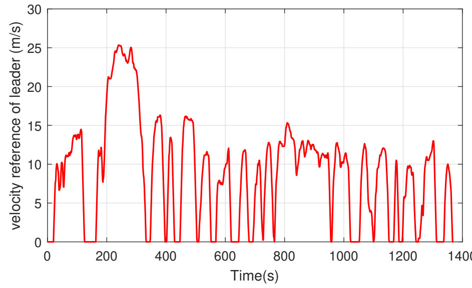

Fig. 5. Urban Dynamometer Driving Schedule (velocity reference)

4.2 Platooning based on ACC system

For ACC platoon whose followers contain LQR controllers, the signals obtained through simulation are observed in the next figures as follows:

- Fig.6a depicted the car velocities with zoom in specific area.
- Fig.6b illustrates the inter-car spacing between two successive cars pairs.
- Fig.6c contains the spacing errors as being the difference between the real spacing and the desired inter-car spacing.
- In Fig.6d the velocity errors as being the difference between the real velocity and the leader's velocity reference

The platoon tracking trajectories in terms of car velocities, velocity errors to the leader car, the inter-car spacing and spacing errors between two successive cars pairs are presented in Fig.6c. It is clearly shown that the car platoon under the ACC strategy successfully achieves the desired spacing and maintains the desired velocity of the leading car. To further observe the attenuation of the spacing errors, Fig.6c – right zoom are shown. We can find that the spacing errors are not amplified propagating the platoon upstream (i.e., $|\varepsilon_1| \ge |\varepsilon_2\| \ge \ldots \ge \|\varepsilon_7\| \ge \|\varepsilon_8\|$), which is also in good agreement with the results of the previous stability analysis.

4.3 Platooning based on CACC system

In the case of CACC platoon implemented with LQR controllers for followers, the signals resulted after simulation can be presented as follows:

- The car velocities are illustrated in Fig.7a, in which can be seen that they follow the velocity profile introduced as the leader's velocity reference.
- Fig.7b contains the spacings between two successive cars pairs during their movement.
- The spacing errors obtained in this simulation case can be viewed in Fig.7c.
- The velocity errors as being the difference between the real velocity and the leader's velocity reference is depicted in Fig.7d.

In each figure there are zooms on specific areas that can help to easily analyse the results.

In Fig.7a, the velocities of all car in the platooning are relatively consistent, which illustrates that the whole platoon drives forward stably under the guidance of the leader car.

In Fig.7b, 7c, 7d, the driving behaviour of the leader car consists continuous acceleration and deceleration, velocity errors, the

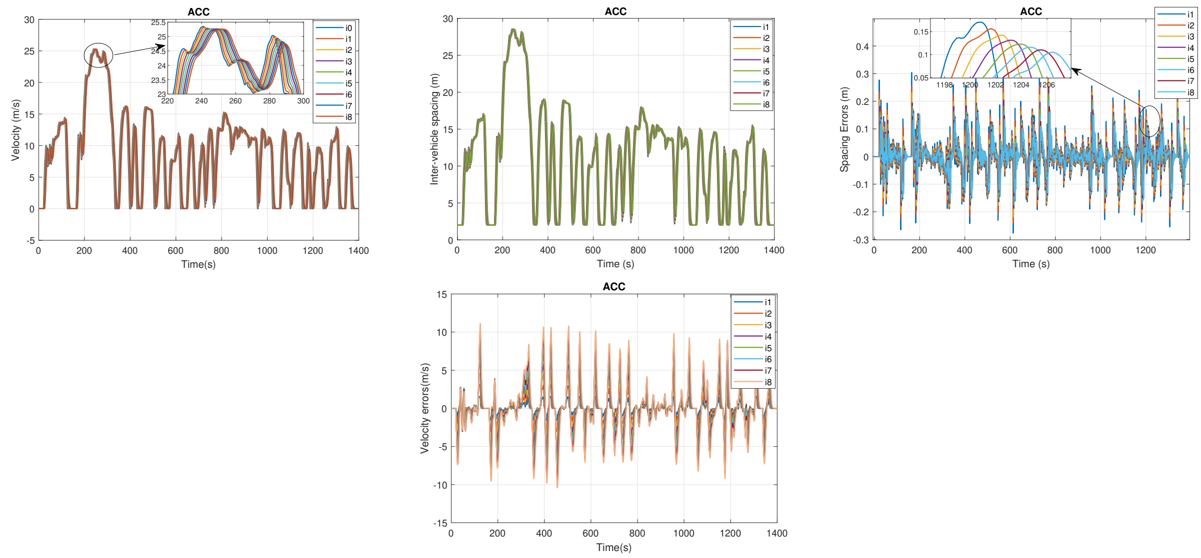

Fig. 6. Platoon response under ACC system based on CTH Strategy

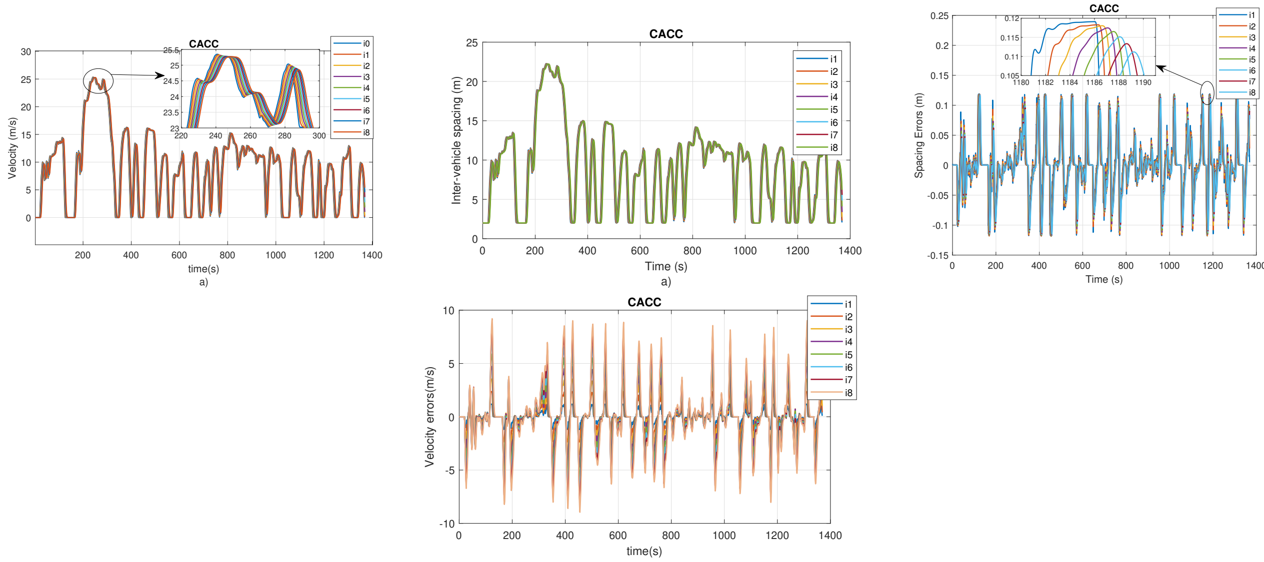

Fig. 7. Platoon response under CACC system based on CTH Strategy With PF Scheme

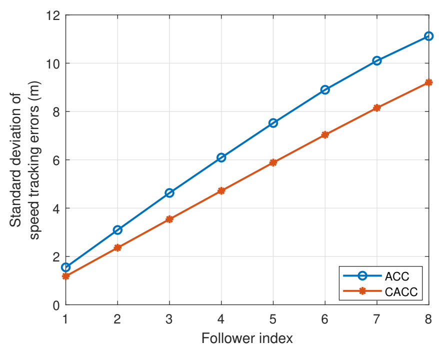

Fig. 8. Comparison of speed errors over the ACC system, CACC system under CTH Strategy

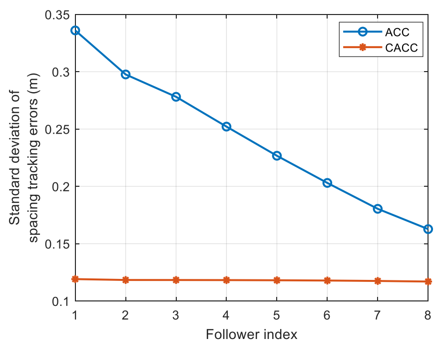

Fig. 9. Comparison of distance errors over the ACC system, CACC system under CTH Strategy

inter-car spacing and spacing errors between two successive cars pairs in the platoon are adjusted with the adjustment of the driving behaviour of the leader car, so as to always maintain the stability of the platoon.

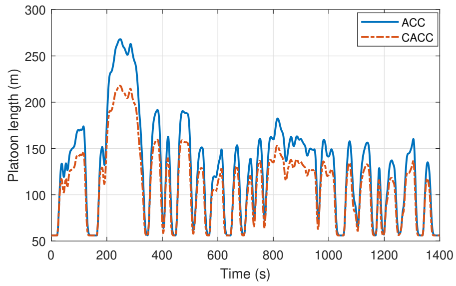

Fig. 10. Comparison of platoon length over the ACC system, CACC system under CTH Strategy

Therefore, Fig.7 generally reflects that CACC controller can conduct safe and stable longitudinal control under CTH Strategy which is also in good agreement with the results of the previous stability analysis.

4.4 Comparison results in control performance

To demonstrate the communication efficiency of CACC controller based on CTH Strategy. It is observed that the spacing errors of each follower in ACC platoon is respectively generally larger than CACC platoon. Specifically, from Fig.8, 9 that standard deviation of speed tracking errors and standard deviation of spacing tracking errors of ACC platoon are larger than CACC system.

Compared with platoon length, it is obvious from Fig.10 that platoon length of CACC platoon is smaller than ACC system, which implies better traffic throughput improvement in this case i.e., CACC platoon increasing the urban arterial capacity better than ACC platoon.

From the result analysis demonstrates that the CACC platoon performance and behavior become better than ACC platoon due to benefits of V2V Communication on time headway for Autonomous and Connected cars. The simulation results did demonstrate superiority compared to other related studies, such as in Luu et al. (2022), Luu et al. (2019).

5. CONCLUSIONS

In this paper, we have considered the benefits of employing information obtained throught V2V communication on the performance of the autonomous platoons. The simulation results show both ACC vehicular platoon, CACC vehicular platoon using the CTH Strategy are always guaranteed "string stability" based on the infinity norm of the error propagation transfer function and Nyquist diagram provide a sufficient condition that guarantees internal stability. However, the CACC vehicular platoon with information from 'r' predecessor cars that the platoon allows the use of smaller time headway values and both performance, behavior are better, therefore increasing the traffic capacity.

Loss of traffic data has not been considered in this paper and the loss of traffic data in the platoon may affect the performance of the CACC system. Hence, a possible future direction would be to explore packet loss.

ACKNOWLEDGEMENTS

This work was supported by The University of Danang-University of Science and Technology, code number of Project: T2023-02-26. The authors would like to thank the support of this institution.

REFERENCES

Barooah, P. and Hespanha, J.P. (2005). Error amplification and disturbance propagation in vehicle strings with decentralized linear control. In *Proceedings of the 44th IEEE conference on Decision and Control*, 4964–4969. IEEE.

Darbha, S., Konduri, S., and Pagilla, P.R. (2020). Vehicle platooning with constant spacing strategies and multiple vehicle look ahead information. *IET Intelligent Transport Systems*, 14(6), 589–600.

Fahad, M. and Nagy, R. (2023). Truck platoon analysis for autonomous trucks. *SN Applied Sciences*, 5(5), 143.

Feng, S., Zhang, Y., Li, S.E., Cao, Z., Liu, H.X., and Li, L. (2019). String stability for vehicular platoon control: Definitions and analysis methods. *Annual Reviews in Control*, 47, 81–97.

Ghasemi, A., Kazemi, R., and Azadi, S. (2013). Stable decentralized control of a platoon of vehicles with heterogeneous information feedback. *IEEE Transactions on Vehicular Technology*, 62(9), 4299–4308.

Godbole, D.N. and Lygeros, J. (1994). Longitudinal control of the lead car of a platoon. *IEEE Transactions on Vehicular Technology*, 43(4), 1125–1135.

Guo, G. and Yue, W. (2012). Autonomous platoon control allowing range-limited sensors. *IEEE Transactions on vehicular technology*, 61(7), 2901–2912.

Guo, G. and Yue, W. (2014). Sampled-data cooperative adaptive cruise control of vehicles with sensor failures. *IEEE Transactions on Intelligent Transportation Systems*, 15(6), 2404–2418.

He, D. and Peng, B. (2020). Gaussian learning-based fuzzy predictive cruise control for improving safety and economy of connected vehicles. *IET Intelligent Transport Systems*, 14(5), 346–355.

Li, S.E., Qin, X., Li, K., Wang, J., and Xie, B. (2017). Robustness analysis and controller synthesis of homogeneous vehicular platoons with bounded parameter uncertainty. *IEEE/ASME Transactions on Mechatronics*, 22(2), 1014–1025.

Li, X., Xu, W., Wang, T., and Yuan, Y. (2022). Infrastructure enabled eco-approach for transit system: A simulation approach. *Transportation Research Part D: Transport and Environment*, 106, 103265.

Li, Z., Hu, B., Li, M., and Luo, G. (2019). String stability analysis for vehicle platooning under unreliable communication links with event-triggered strategy. *IEEE Transactions on Vehicular Technology*, 68(3), 2152–2164.

Luu, D.L. and Lupu, C. (2019). Dynamics model and design for adaptive cruise control vehicles. In *2019 22nd International Conference on Control Systems and Computer Science (CSCS)*, 12–17. IEEE.

Luu, D.L., Lupu, C., and Van Nguyen, T. (2019). Design and simulation implementation for adaptive cruise control systems of vehicles. In *2019 22nd International Conference on Control Systems and Computer Science (CSCS)*, 1–6. IEEE, Romania.

Luu, L.D., Lupu, C., and Alshareefi, H.D. (2022). A comparative study of adaptive cruise control system based on different spacing strategies. *Journal of Control Engineering and Applied Informatics*, 24(2), 3–12.

Mokogwu, C.N. and Hashtrudi-Zaad, K. (2022). Energy-based analysis of string stability in vehicle platoons. *IEEE Transactions on Vehicular Technology*, 71(6), 5915–5929.

Nowakowski, C., Thompson, D., Shladover, S.E., Kailas, A., and Lu, X.Y. (2016). Operational concepts for truck maneuvers with cooperative adaptive cruise control. *Transportation Research Record*, 2559(1), 57–64.

Öncü, S., Ploeg, J., Van de Wouw, N., and Nijmeijer, H. (2014). Cooperative adaptive cruise control: Network-aware analysis of string stability. *IEEE Transactions on Intelligent Transportation Systems*, 15(4), 1527–1537.

Orosz, G. (2016). Connected cruise control: modelling, delay effects, and nonlinear behaviour. *Vehicle System Dynamics*, 54(8), 1147–1176.

Pi, D., Xue, P., Wang, W., Xie, B., Wang, H., Wang, X., and Yin, G. (2023). Automotive platoon energy-saving: A review. *Renewable and Sustainable Energy Reviews*, 179, 113268.

Ploeg, J., Shukla, D.P., Van De Wouw, N., and Nijmeijer, H. (2013). Controller synthesis for string stability of vehicle platoons. *IEEE Transactions on Intelligent Transportation Systems*, 15(2), 854–865.

Rajamani, R. (2011). *Vehicle dynamics and control*. Springer Science & Business Media, London.

Stankovic, S.S., Stanojevic, M.J., and Siljak, D.D. (2000). Decentralized overlapping control of a platoon of vehicles. *IEEE Transactions on Control Systems Technology*, 8(5), 816–832.

Swaroop, D., Hedrick, J.K., and Choi, S.B. (2001). Direct adaptive longitudinal control of vehicle platoons. *IEEE transactions on vehicular technology*, 50(1), 150–161.

Tan, H.S., Rajamani, R., and Zhang, W.B. (1998). Demonstration of an automated highway platoon system. In *Proceedings of the 1998 American control conference. ACC (IEEE Cat. No. 98CH36207)*, volume 3, 1823–1827. IEEE.

Tiganasu, A., Lazar, C., Caruntu, C.F., and Dosoftei, C. (2021). Comparative analysis of advanced cooperative adaptive cruise control algorithms for vehicular cyber physical systems. *Journal of Control Engineering and Applied Informatics*, 23(1), 82–92.

Turan, A. (2024). Pid controller design with a new method based on proportional gain for cruise control system. *Journal of Radiation Research and Applied Sciences*, 17(1), 100810.

Varaiya, P. (1993). Smart cars on smart roads: problems of control. *IEEE Transactions on automatic control*, 38(2), 195–207.

Wang, Y., Wang, S., Su, C., Li, X., Zhang, Q., Zhang, Z., and Tian, M. (2024). Car-following stability improvement of cooperative adaptive cruise control based on distributed model predictive control. *Proceedings of the Institution of Mechanical Engineers, Part D: Journal of Automobile Engineering*, 09544070231211377.

Wu, C., Xu, Z., Liu, Y., Fu, C., Li, K., and Hu, M. (2020). Spacing policies for adaptive cruise control: A survey. *IEEE Access*, 8, 50149–50162.

Wu, Z., Sun, J., and Xu, R. (2021). Consensus-based connected vehicles platoon control via impulsive control method. *Physica A: Statistical Mechanics and its Applications*, 580, 126190.

Yanakiev, D. and Kanellakopoulos, I. (1998). Nonlinear spacing policies for automated heavy-duty vehicles. *IEEE Transactions on Vehicular Technology*, 47(4), 1365–1377.

Zhang, Y., Wang, M., Hu, J., and Bekiaris-Liberis, N. (2020). Semi-constant spacing policy for leader-predecessor-follower platoon control via delayed measurements synchronization. *IFAC-PapersOnLine*, 53(2), 15096–15103.

Zhang, Z., Li, X., Su, C., Liu, X., Xiong, X., Xiao, T., and Wang, Y. (2023). Potential field-based cooperative adaptive cruising control for longitudinal following and lane changing of vehicle platooning. *Physica A: Statistical Mechanics and its Applications*, 632, 129317.

Zhou, S., Walker, P., and Zhang, N. (2020). Parametric design and regenerative braking control of a parallel hydraulic hybrid vehicle. *Mechanism and Machine Theory*, 146, 103714.

Appendix A. PROOF OF THEOREM 1

Substituting $s = j\omega$ into the transfer function (27), one can have:

$$|\Phi_i(j\omega,\theta)|^2 \triangleq \frac{N}{D} \tag{45}$$

where

$$\begin{aligned} N &= \kappa_1^2 - \kappa_2^2\omega^2, \\ D &= [\kappa_1 - (1-\kappa_3)\omega^2]^2 + [(\kappa_2 + h_i\kappa_1) - \varsigma_i\omega^2]^2\omega^2. \end{aligned} \tag{46}$$

we obtain that the inequality in (36), if

$$\begin{aligned} D - N = \varsigma_i^2\omega^6 + [(1-\kappa_3)^2 - 2\varsigma_i(\kappa_2 + h_i\kappa_1)]\omega^4 + [(\kappa_2 + h_i\kappa_1)^2 \\ - 2\kappa_1(1-\kappa_3) - \kappa_2^2]\omega^2 \geq 0 \end{aligned} \tag{47}$$

$$\begin{aligned} \Rightarrow \varsigma_i^2\omega^4 + [(1-\kappa_3)^2 - 2\varsigma_i(\kappa_2 + h_i\kappa_1)]\omega^2 + h_i^2\kappa_2^2 \\ + 2\kappa_1\kappa_2 h_i - 2\kappa_1 + 2\kappa_1\kappa_3 \geq 0 \end{aligned} \tag{48}$$

Defining $\kappa_1 = \frac{\lambda}{h_i}$, $\kappa_2 = \frac{1}{h_i}$, the inequality (48) become as follows:

$$\Rightarrow \varsigma_i^2\omega^4 + [(1-\kappa_3)^2 - 2\varsigma_i(\frac{1}{h_i} + \lambda)]\omega^2 + h_i^2\kappa_2^2 + 2\kappa_1\kappa_3 \geq 0 \tag{49}$$

The inequality (49) are satisfied, when

$$\begin{aligned} &\kappa_1\kappa_3 \geq 0 \Rightarrow \kappa_3 \geq 0 \\ &(1-\kappa_3)^2 - 2\varsigma_i(\frac{1}{h_i} + \lambda) \geq 0. \Rightarrow h_i \geq \frac{2\varsigma_i}{(1-\kappa_3)^2 - 2\varsigma_i\lambda} \end{aligned} \tag{50}$$

This is possible for $\lambda << 0$, we can deduce that

$$h_i \geq h_{min} = \frac{2\varsigma_i}{(1-\kappa_3)^2} \tag{51}$$

Appendix B. PROOF OF THEOREM 2

Substituting $s = j\omega$ into the transfer function (33), one can have:

$$|\tilde{\Phi}_i(j\omega,\theta)|^2 \triangleq \frac{\tilde{N}}{\tilde{D}} \tag{52}$$

where

$$\begin{aligned} &\tilde{N} = (\tilde{\kappa}_1 - \tilde{\kappa}_3\omega^2)^2 + \tilde{\kappa}_2^2\omega^2 \\ &\tilde{D} = (-\omega^2 - \tilde{\kappa}_1\omega^2 cos(\theta\omega) + [\tilde{\kappa}_2 + \tilde{\kappa}_1 h_i)\omega sin(\theta\omega) + \tilde{\kappa}_1 cos(\theta\omega)] \\ &+ [-\varsigma_i\omega^3 + \tilde{\kappa}_1\omega^2 sin(\theta\omega) + (\tilde{\kappa}_2 + \tilde{\kappa}_1 h_i)\omega cos(\theta\omega) - \tilde{\kappa}_1 sin(\theta\omega)]^2 \end{aligned} \tag{53}$$

After some simplifications, we have

$$\tilde{D}-\tilde{N} = M_6\omega^6 + M_5\omega^5 + M_4\omega^4 + +M_3\omega^3 + M_2\omega^2 \geq 0 \tag{54}$$

where

$$M_6 = \varsigma_i^2,$$
$$M_5 = -2\varsigma_i\tilde{\kappa}_1 sin(\theta\omega),$$
$$M_4 = 1+2[\tilde{\kappa}_2 - \varsigma_i(\tilde{\kappa}_2\tilde{\kappa}_1 h_i)]cos(\theta\omega),$$
$$M_3 = 2[\tilde{\kappa}_1(\varsigma_i - h_i) - \tilde{\kappa}_2]sin(\theta\omega),$$
$$M_2 = \tilde{\kappa}_1^2 h_i^2 + 2\tilde{\kappa}_1\tilde{\kappa}_2 h_i - 2\tilde{\kappa}_1 cos(\theta\omega).$$

Considering the fact that $sin(\theta\omega) \leq \theta\omega$ for $\omega \geq 0$ and $cos(\theta\omega) \leq 1$ and also considering

$$\tilde{\kappa}_1(\varsigma_i - h_i) - \tilde{\kappa}_2 \leq 0 \tag{55}$$

if

$$\tilde{\kappa}_3 - \varsigma_i(\tilde{\kappa}_2 + \tilde{\kappa}_1 h_i) \leq 0 \tag{56}$$

then we need to have

$$\tilde{D}-\tilde{N} \geq \omega^2(\tilde{M}_4\omega^4 + \tilde{M}_2\omega^2 + \tilde{M}_0), \tag{57}$$

where

$$\tilde{M}_4 = \varsigma_i^2 - 2\varsigma_i\tilde{\kappa}_3\theta,$$
$$\tilde{M}_2 = 1+2[\tilde{\kappa}_3 - \varsigma_i(\tilde{\kappa}_2 + \tilde{\kappa}_1 h_i)] + 2\theta[\tilde{\kappa}_1(\varsigma_i - h_i) - \tilde{\kappa}_2],$$
$$\tilde{M}_0 = \tilde{\kappa}_1^2 h_i^2 + 2\tilde{\kappa}_1\tilde{\kappa}_2 h_i - 2\tilde{\kappa}_1.$$

Having $\tilde{M}_4, \tilde{M}_2, \tilde{M}_0 \geq 0$, this leads to string stability. Therefore, there are three cases as follows:

$$\tilde{M}_4 \geq 0 \Rightarrow \tilde{\kappa}_3 \leq \frac{\varsigma_i}{2\theta},$$
$$\tilde{M}_2 \leq 0 \Rightarrow \tilde{\kappa}_2 \leq \frac{1+2\tilde{\kappa}_3 + 2\tilde{\kappa}_1(\varsigma_i\theta - \theta h_i - \varsigma_i h_i)}{2(\varsigma_i + \theta)},$$
$$\tilde{M}_0 \geq 0 \Rightarrow \tilde{\kappa}_2 \geq \frac{1}{h_i} - \frac{\tilde{\kappa}_1 h_i}{2}.$$

then, we obtain

$$\frac{1}{h_i} - \frac{\tilde{\kappa}_1 h_i}{2} \leq \tilde{\kappa}_2 \leq \frac{1+2\tilde{\kappa}_3 + 2\tilde{\kappa}_1(\varsigma_i\theta - \theta h_i - \varsigma_i h_i)}{2(\varsigma_i + \theta)}$$

The above inequality means that

$$\frac{1+2\tilde{\kappa}_3 + 2\tilde{\kappa}_1(\varsigma_i\theta - \theta h_i - \varsigma_i h_i)}{2(\varsigma_i + \theta)} - \frac{1}{h_i} + \frac{\tilde{\kappa}_1 h_i}{2} \geq 0$$

After some simplifications, we achieve:

$$\frac{h_i(1+2\tilde{\kappa}_3) - 2(\varsigma_i + \theta) + h_i\tilde{\kappa}_1(2\varsigma_i\theta - \theta h_i - \varsigma_i h_i)}{2h_i(\varsigma_i + \theta)} \geq 0$$

Then, by assuming $2\varsigma_i\theta - \theta h_i - \varsigma_i h_i \leq 0$ and given that the control gains are positive, it is evident that:

$$h_i(1+2\tilde{\kappa}_3) - 2(\varsigma_i + \theta) \geq 0$$

Therefore, the lower bound for the time headway can be determined as:

$$h_i \geq h_{min} = \frac{2(\varsigma_i + \theta)}{1+2\tilde{\kappa}_3}.$$